

Calcite–graphite isotope thermometry in amphibolite facies marble, Bancroft, Ontario

S. R. DUNN

Department of Earth and Environment, Mount Holyoke College, South Hadley, MA 01075, USA (sdunn@mtholyoke.edu)

ABSTRACT This study presents calcite–graphite carbon isotope fractionations for 32 samples from marble in the northern Elzevir terrane of the Central Metasedimentary Belt, Grenville Province, southern Ontario, Canada. These results are compared with temperatures calculated by calcite–dolomite thermometry (15 samples), garnet–biotite thermometry (four samples) and garnet–hornblende thermometry (three samples). $\Delta_{\text{cal-gr}}$ values vary regularly across the area from $>6.5\text{‰}$ in the south to 4.0‰ in the north, which corresponds to temperatures of 525 °C in the south to 650 °C in the north. Previous empirical calibration of the calcite–graphite thermometer agrees very well with calcite–dolomite, garnet–biotite and garnet–hornblende thermometry, whereas, theoretical calibrations compare less well with the independent thermometry. Isograds in marble based on the reactions rutile + calcite + quartz = titanite and tremolite + calcite + quartz = diopside, span temperatures of $525\text{--}600\text{ °C}$ and are consistent with calculated temperature– $X(\text{CO}_2)$ relations. Results of this study compare favourably with large-scale regional isotherms, however, local variation is greater than that revealed by large-scale sampling strategies. It remains unclear whether the temperature– $\Delta_{\text{cal-gr}}$ relationship observed in natural materials below 650 °C represents equilibrium fractionations or not, but the regularity and consistency apparent in this study demonstrate its utility for thermometry in amphibolite facies marble.

Key words: calcite; carbon isotopes; geothermometry; graphite; Grenville Province.

INTRODUCTION

The partitioning of carbon isotopes between calcite and graphite in metamorphic rocks has been successfully employed as a geothermometer, especially in high-temperature marble (Valley, 2001 and references therein). At temperatures below *c.* 600 °C , calibration uncertainty and likely disequilibrium between calcite and graphitized organic pre-cursor render this system of questionable reliability. The purpose of this study is to show that calcite–graphite $^{13}\text{C}/^{12}\text{C}$ fractionations can provide accurate thermometry results in amphibolite facies marble to temperatures as low as $525\text{--}550\text{ °C}$ when compared with results of calcite–dolomite, garnet–biotite and garnet–hornblende thermometry.

Isotopic thermometers are analogous to cation-exchange thermometers and subject to the same potential problems, including the attainment and retention of peak metamorphic conditions, modification by diffusion and exchange during cooling, uncertainties or errors in calibration and analytical uncertainty. Cation exchange and net transfer reaction thermometers have additional uncertainties imposed by mineral activity models (e.g. Essene, 1989; Kohn & Spear, 1991). Ideally, a geothermometer should yield self-consistent results that compare favourably with other geothermometers and with regional mineral

equilibria. This study shows that the calcite–graphite thermometer can provide such results in amphibolite facies rocks.

Rathmell *et al.* (1999) compared calcite–graphite, calcite–dolomite and garnet–biotite thermometry over a large region that includes the present study area and thus provides an important regional context for these new results. In contrast to the present study, Rathmell *et al.* (1999) found significant differences in regional isotherms based on the different geothermometers. Despite large differences in sampling density and distance scales, both studies conclude that the calcite–graphite system is a particularly useful thermometer in this geological terrane.

THE CALCITE–GRAPHITE THERMOMETER

The temperature-sensitive $^{12}\text{C}\text{--}^{13}\text{C}$ exchange between calcite and graphite constitutes an important thermometer in marble (Valley, 2001). Many potential thermometers, especially stable isotope systems, must be applied with caution because exchange by diffusion or recrystallization can result in partial or complete resetting during cooling. If there has been no recrystallization, then diffusion rates and grain size/shape allow one to model retrograde exchange and permit peak temperatures to be backed out from measured fractionations (e.g. Dodson, 1973; Giletti, 1986; Eiler

et al., 1992; Farquhar *et al.*, 1993). However, diffusion modelling is unnecessary when the exchange component of interest involves only two minerals and one is a refractory accessory mineral (RAM thermometer of Valley, 2001). In such a system, the slow diffusing mineral is below its closure temperature for exchange by diffusion and the fast diffusing mineral thus has no other phase to exchange with. Graphite-bearing calcite marbles are ideal candidates for calcite–graphite thermometry as relatively small amounts of refractory graphite are disseminated in a large reservoir of calcite. Small amounts of dolomite or scapolite may be present in calcite marble, however, calcite–dolomite and calcite–scapolite $^{13}\text{C}/^{12}\text{C}$ fractionations are small (Sheppard & Schwarcz, 1970; Moecher *et al.*, 1994) and can be ignored when a relatively small proportion of the carbon is contained in these phases. The presence of other silicate minerals has no effect as they do not contain appreciable carbon.

The self-diffusion of carbon in graphite is exceedingly slow (Thrower & Mayer, 1978), especially when compared with calcite (Labotka *et al.*, 2004). Although graphite is highly anisotropic, self-diffusion within graphite is approximately isotropic with a pre-exponential diffusion constant (D_0) of $9.1 \times 10^{-5} \text{ m}^2 \text{ s}^{-1}$ and diffusion energy (E) of 656 kJ mol^{-1} (Thrower & Mayer, 1978). Thus, carbon diffusion in graphite is orders of magnitude slower than cation diffusion in silicate minerals, much slower even than coupled diffusion such as CaAl–NaSi in plagioclase (see Brady, 1995). Dodson (1973) closure temperatures for carbon diffusion in graphite are over $1100 \text{ }^\circ\text{C}$ even for $1 \text{ }\mu\text{m}$ grains at extremely slow cooling rates of $1 \text{ }^\circ\text{C Myr}^{-1}$. Thus, graphite has no opportunity for isotopic homogenization by intracrystalline diffusion even in granulite facies metamorphic rocks. Isotopic homogenization may occur, however, by recrystallization processes such as dissolution/reprecipitation and coarsening.

Coarse flakes of graphite from granulite facies terranes sometimes exhibit isotopic zoning from core-to-rim (Wada, 1988; Arita & Wada, 1990; Santosh & Wada, 1993; Kitchen & Valley, 1995; Farquhar *et al.*, 1999; Satish-Kumar, 2000; Satish-Kumar & Wada, 2000; Satish-Kumar *et al.*, 2002). When present, zoning is most often consistent with formation of graphite overgrowths involving a fluid phase during retrograde conditions. Possible preservation of prograde zoning is also seen, but rarely. The cores of graphite grains in these studies are most often isotopically homogeneous, or nearly so, and because carbon self-diffusion is ineffective, isotopic homogeneity is not likely to come about by intracrystalline diffusion. Graphite recrystallization coincident with prograde coarsening (Ostwald ripening) is the most likely cause of homogeneous $^{13}\text{C}/^{12}\text{C}$ ratios in graphite grains from high-grade terranes and, thus, calcite–graphite thermometry on whole-rock materials in those cases will yield peak metamorphic temperatures.

Thermometer calibrations

The temperature dependence of $\Delta_{\text{cal-gr}}$ has been explored by experimental methods (Scheele & Hoefs, 1992), theoretical methods (Bottinga, 1969; Chacko *et al.*, 1991; Polyakov & Kharlashina, 1995) and empirical methods (Valley & O'Neil, 1981; Wada & Suzuki, 1983; Morikiyo, 1984; Dunn & Valley, 1992; Kitchen & Valley, 1995). ($\Delta_{\text{cal-gr}} = \delta^{13}\text{C}_{\text{calcite}} - \delta^{13}\text{C}_{\text{graphite}}$, standard δ -notation, $\delta^{13}\text{C}_{\text{A}\text{‰}} = [((^{13}\text{C}/^{12}\text{C})_{\text{A}} / (^{13}\text{C}/^{12}\text{C})_{\text{std}}) - 1] \times 10^3$, PDB standard.) All studies are consistent with the conclusion that isotopic exchange in the system is limited by exceedingly slow diffusion rates in graphite. Unfortunately, the slow diffusion rates in graphite have made experimental determination of equilibrium carbon isotopic fractionations ($\Delta_{\text{cal-gr}}$) difficult. The only published experimental study for graphite (Scheele & Hoefs, 1992) is not consistent with theoretical or empirical findings. These experiments involve only partial exchange (CO_2 –graphite). They did not reverse the $^{13}\text{C}/^{12}\text{C}$ fractionation and did not attain equilibrium. Application of the Scheele & Hoefs (1992) calibration to natural calcite–graphite pairs from granulite facies rocks yield temperatures typically in excess of $1000 \text{ }^\circ\text{C}$ and often above $1200 \text{ }^\circ\text{C}$, yet no evidence such as wide-scale melting supports such extreme regional temperatures in these terranes (Morrison & Barth, 1993; Kitchen & Valley, 1995; Valley, 2001).

Calibration of the calcite–graphite fractionation is only a problem for thermometry in metamorphic rocks below $650 \text{ }^\circ\text{C}$ (Fig. 1). Above that, the empirical calibration of Kitchen & Valley (1995) gives excellent results that agree well with the theoretical calibrations of Chacko *et al.* (1991) and Polyakov & Kharlashina (1995) (see also Satish-Kumar & Wada, 2000). At temperatures below $650 \text{ }^\circ\text{C}$, empirical calibrations begin to diverge sharply from theoretical calibrations

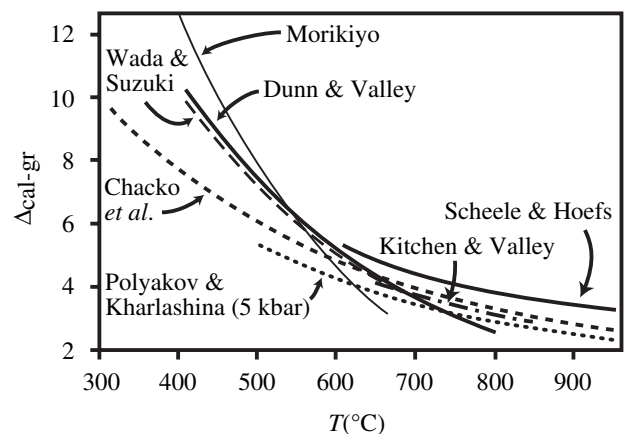


Fig. 1. Temperature dependence of $\Delta^{13}\text{C}_{\text{cal-gr}}$ proposed by various workers discussed in text. Polyakov & Kharlashina (1995) is shown for 500 MPa. Decreasing pressure shifts $\Delta_{\text{cal-gr}}$ values slightly upward.

towards larger $\Delta_{\text{cal-gr}}$ values (see Chacko *et al.*, 1991; Dunn & Valley, 1992). Chacko *et al.* (1991) concluded that all natural data represent disequilibrium below temperatures of *c.* 650 °C. This is consistent with exceedingly slow diffusion rates in graphite and incomplete isotopic exchange with calcite at metamorphic temperatures below the upper amphibolite facies.

Dunn & Valley (1992) interpreted scatter in $\Delta_{\text{cal-gr}}$ values within the greenschist facies as probably because of incomplete graphitization and incomplete isotopic equilibration of the protolith organic matter. High-resolution transmission electron microscope images of 'graphitic' material by Buseck & Huang (1985) show progressive graphite crystallization in the greenschist facies. Particle rims become highly organized while interiors remain structurally immature. Dunn & Valley (1992) suggest equilibrium calcite–graphite $^{13}\text{C}/^{12}\text{C}$ fractionations will apply only to fully graphitized portions of such grains and thus bulk analyses scatter towards larger $\Delta_{\text{cal-gr}}$ values. Graphitization appears to reach completion in the upper greenschist facies (garnet zone, $T \cong 500$ °C), but it remains unclear whether or not equilibrium isotopic exchange is attained as graphitization reaches completion. If prograde isotopic zoning exists, comparable to cation zoning in garnet and other silicates, then bulk analyses will underestimate the final growth temperature. However, if graphite grains continually recrystallize as they coarsen, then isotopic equilibrium might be maintained as coarsening proceeds.

Whether or not calcite–graphite $^{13}\text{C}/^{12}\text{C}$ fractionations represent equilibrium below 650 °C, they have been shown to accurately represent metamorphic conditions when compared with other temperature-sensitive equilibria. Several studies have concluded that the calibration of Dunn & Valley (1992) provides accurate temperature determinations in upper greenschist to amphibolite facies marbles (Morrison & Barth, 1993; Bergfeld *et al.*, 1996; Satish-Kumar *et al.*, 1997; Rathmell *et al.*, 1999; this study). Disequilibrium $^{13}\text{C}/^{12}\text{C}$ fractionations in bulk calcite and graphite could yield reliable temperature information if graphite routinely deviates from equilibrium in a consistent manner. This could result, for example, if graphite coarsening produces isotopic zoning in a consistent way regardless of heating rates.

The question of equilibrium *v.* disequilibrium isotopic fractionation in calcite–graphite pairs awaits size fraction or ion microprobe efforts. The best method for thermometry at present appears to be the empirical calibrations of Kitchen & Valley (1995) for temperatures above *c.* 650 °C and Dunn & Valley (1992) below *c.* 650 °C.

Caution should be exercised in applying calcite–graphite thermometry to rocks in the amphibolite facies and below because scatter in $\Delta_{\text{cal-gr}}$ values is observed and presumed to result from failure of graphitic material to fully equilibrate with calcite.

Also, bulk graphite analyses from samples that contain abundant silicate minerals are potentially problematic as graphite enclosed within silicate minerals have been shown to have lower temperature $^{13}\text{C}/^{12}\text{C}$ fractionations than the graphite hosted within calcite (Wada & Suzuki, 1983; Dunn & Valley, 1992). Similarly, Bergfeld *et al.* (1996) found that calcite–graphite pairs from graphitic schist dominated by silicate minerals generally give lower temperature fractionations than those from graphitic marble at the same grade. This may result either from silicate armouring of graphite or modification of calcite after peak metamorphism. With this in mind, application of this thermometer should be restricted to calcite-rich marble whenever possible.

GEOLOGICAL SETTING

The study area is located within the northern portion of the Belmont domain (Elzevir terrane) of the Central Metasedimentary Belt, Grenville Province, Ontario. This domain includes a supracrustal sequence of metamorphosed volcanic rocks and clastic and carbonate sedimentary rocks (deposited *c.* 1300–1250 Ma) intruded by numerous 1245–1229 Ma granitic and gabbroic plutons (Carr *et al.*, 2000; Easton, 2000). Contact aureoles are well developed (1–1.5 km wide) around these intrusions (Lumbers, 1969; Dunn & Valley, 1992, 1996). The abundance of intrusive rocks of this age and the amalgamation of various arcs into a composite terrane at this time suggests that the domain may have experienced a regional thermal event at *c.* 1245 Ma (the Elzevir orogeny of Moore & Thompson, 1980; see also Carr *et al.*, 2000; Easton, 2000). Widespread metamorphism, deformation and igneous activity affected the region again during the main phase of the Ottawa orogeny, 1060–1020 Ma (Mezger *et al.*, 1993; Easton, 2000). This event obscures earlier metamorphism, except immediately adjacent to the larger intrusions.

The Belmont terrane exhibits an increase in metamorphic grade from south to north. Carmichael *et al.* (1978) recognized a sequence of mineral isograds in pelitic rocks indicating a metamorphic low centred just north and west of Madoc, Ontario (Fig. 2). Marble in that area is fine-grained and often banded in shades of gray. Dolomite + quartz is abundant, as are rutile + calcite + quartz assemblages. Mafic rocks in that area contain greenschist facies assemblages of actinolite + albite or oligoclase (sometimes both) + biotite \pm epidote \pm chlorite.

From the latitude of Coe Hill northward (centre of Fig. 2), marble becomes noticeably coarser-grained, commonly still banded, with graphite often visible by hand lens inspection. Tremolite is frequently present and diopside becomes more common approaching Bancroft (northern part of Fig. 2). Within *c.* 5 km south of the latitude of Bancroft, marble is occasionally white, very coarse-grained and massive, similar in all respects to that found within the high-grade Bancroft

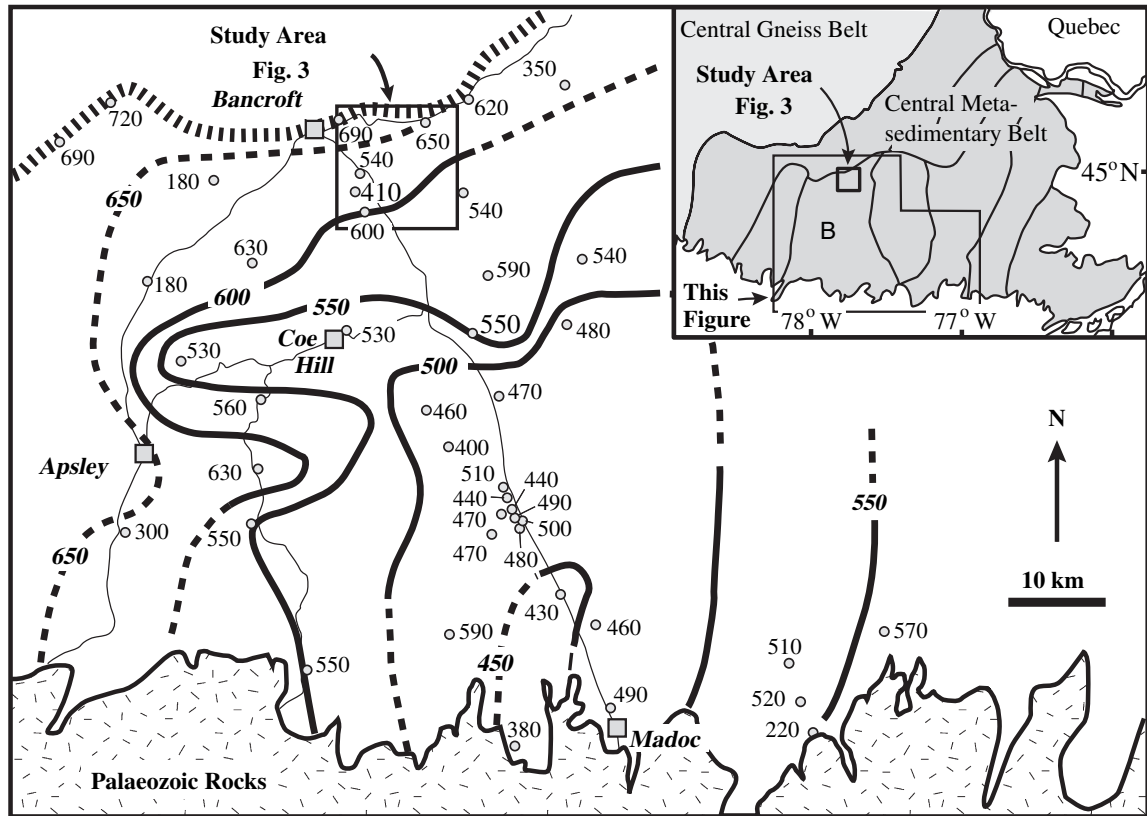


Fig. 2. Regional isotherms and calcite-graphite temperatures from Rathmell *et al.* (1999) with the location of the present study area. Their isotherm placement was also influenced by the Carmichael *et al.* (1978) mineral isograds (not shown). Inset after Easton (2000) shows domains of the Central Metasedimentary Belt (shaded) of southern Ontario, Canada. B, Belmont domain of Elzevir terrane.

terrane, 5 km and more to the north and west. Also at this latitude, calc-silicate rocks, including massive diopside and diopside + tremolite ± scapolite gneiss are sometimes interlayered with marble. Mafic rocks throughout this part of the terrane contain amphibolite facies assemblages of hornblende + intermediate plagioclase + biotite ± garnet ± gedrite.

Regional isotherms based on calcite-graphite isotope thermometry by Rathmell *et al.* (1999) reveal the large-scale thermal structure of the Elzevir terrane (Fig. 2). Rathmell *et al.* (1999) also delineate isotherms based on garnet-biotite and calcite-dolomite thermometry (not shown in Fig. 2). They conclude that the calcite-dolomite solvus results are *c.* 50 °C too low in the Bancroft vicinity, presumably because of resetting during cooling, whereas the garnet-biotite results are in general agreement with calcite-graphite thermometry.

Figure 3 shows the bedrock geology and locations of samples studied. This area was selected for several reasons. First, graphite-bearing marble is abundant and reasonably well exposed, allowing a dense sampling strategy. The average sample spacing is one sample per 2 km² over a roughly 8 × 8 km area. Second, large plutons are absent within the immediate area. Third, regional reconnaissance indicated that marble

in the southern part of this area is generally fine-grained, similar to that in the metamorphic low 40 km to the south. Furthermore, tremolite + calcite + quartz assemblages in the fine-grained marble give way to coarser-grained diopside-bearing marble to the north (Fig. 4). Subsequent thin section study also revealed a transition from rutile + calcite + quartz assemblages in marble from the southern part of this area to titanite-bearing marble northward (Fig. 4). Rutile + calcite + quartz assemblages are common in low-grade (*c.* 500 °C), fine-grained marble from the area to the south (Dunn & Valley, 1996), again suggesting peak temperatures below 600 °C in the southern part of this area. These observations led me to suspect that a larger temperature variation might exist than that indicated by the Rathmell *et al.* (1999) regional isotherms, which show all rocks in the study area attaining metamorphic temperatures of *c.* 600 °C or above.

Sampling strategies

Hundreds of samples were collected throughout the field area and examined in thin section. Thin section chips were stained with alizarin to distinguish calcite from dolomite. Samples selected for calcite-graphite

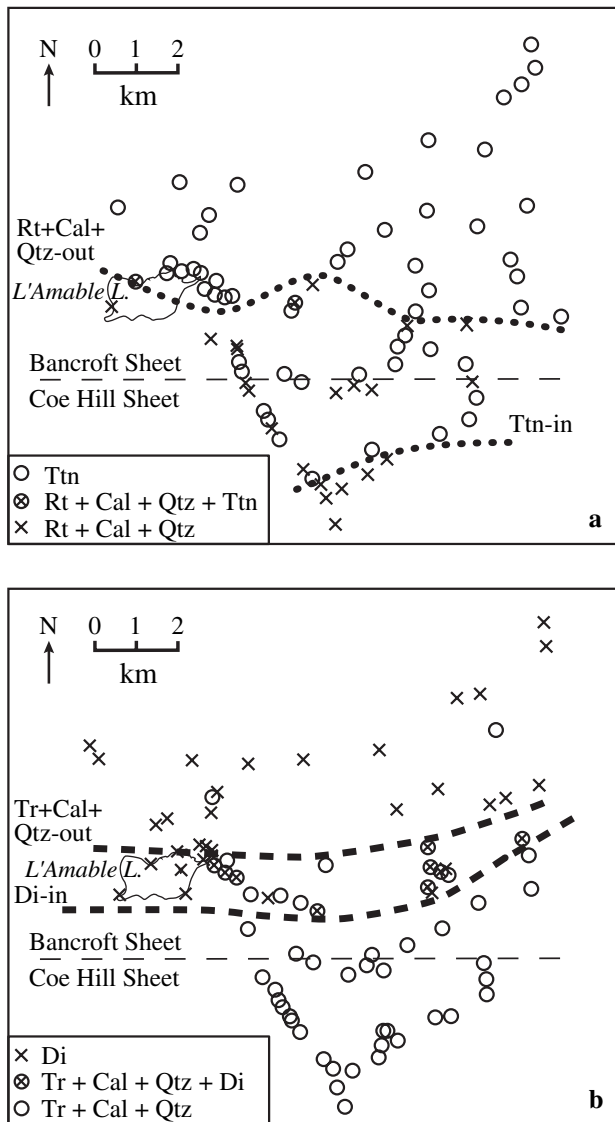


Fig. 4. (a) Occurrence of mineral assemblages in marble relevant to the reaction $\text{rutile} + \text{calcite} + \text{quartz} = \text{titanite} + \text{CO}_2$ and (b) the reaction $\text{tremolite} + 3 \text{calcite} + 2 \text{quartz} = 5 \text{diopside} + 3 \text{CO}_2 + \text{H}_2\text{O}$. Metamorphic grade increases to the north. Samples included in this compilation are not limited to those in Fig. 3.

exsolution features, which also were avoided during analysis.

Care was taken during sample selection to avoid contact metamorphism. All samples are >2 km from the contact aureole of the Umfraville gabbro, which crops out to the south of the study area (south-west corner of Fig. 3). Plutonic rocks are abundant north of the field area within the Bancroft domain, but these are separated from the Belmont domain by a late terrane-bounding extensional fault (heavy dashed line in Fig. 3). Geobarometry indicates a discontinuity of at least 200 MPa across this boundary from pressures of $c. 800$ MPa to the north and <600 MPa in the Elzevir

terrane (Anovitz & Essene, 1990). $^{40}\text{Ar}/^{39}\text{Ar}$ cooling ages are also discontinuous across this boundary and suggest that displacement continued until well after the Ottawa orogeny, perhaps as late as $c. 900$ Ma (Cosca *et al.*, 1992). Thus, the intrusive rocks now exposed north of the field area are not themselves responsible for any thermal affects preserved in the field area, however, if similar plutons were abundant in the overlying rocks (now eroded away), then one would expect higher peak temperatures near the present day fault zone.

The only significant intrusive rocks within the sampling area are a series of concordant metagabbroic sheets that crop out along highway 62, 4 km south of L'Amable Lake (location 86-35 in Fig. 2). A road cut exposes four intrusive sheets that range from 3 to 15 m thick within layered marble and para-amphibolite. These intrusive rocks turn out to coincide with a localized thermal high and most of the gabbro itself has been metamorphosed to garnet amphibolite.

METHODS

Mineral compositions were obtained by wavelength dispersive spectrometry on the Cameca SX-50 electron microprobe at the University of Massachusetts, Amherst, using natural and synthetic mineral standards. Analytical conditions were 15 kV accelerating potential, 15 nA sample current, counting times of 20 s on calcite and 40 s on other minerals and a beam size of $1 \mu\text{m}$ on garnet, $5 \mu\text{m}$ on biotite and hornblende and $15 \mu\text{m}$ on calcite. Oxide weight per cents were calculated with Cameca software, which uses the PAP correction for matrix effects, and OH and CO_2 were determined from stoichiometry. Tests on calcite showed no measurable specimen damage in 20-s analyses with a $15\text{-}\mu\text{m}$ beam.

X-ray maps of garnet assisted in selecting appropriate analytical traverses and points. Garnet compositions are typically homogeneous in their interiors, or show only slight prograde zoning, and all show retrograde zoning within $c. 100 \mu\text{m}$ of rims with an increase in Mn and Fe and decrease in Mg. Garnet analyses were selected for thermometry at the minimum Fe/Mg ratio, just interior to the retrograde zoning. Chemical zoning is not observed in either biotite or hornblende. Matrix grains of these minerals (removed from the garnet) were analysed to avoid possible effects of retrograde exchange as discussed by Tracy (1982) and Spear (1991). Backscattered electron images were used to select homogeneous calcite grains or areas of grains free of dolomite exsolution features to analyse for calcite–dolomite thermometry. Multiple spots were analysed and averaged.

The calcite–dolomite geothermometer of Anovitz & Essene (1987) was applied, which accounts for Fe as well as Mg in calcite. The formulation of Graham & Powell (1984) was used for garnet–hornblende thermometry and Holdaway (2000) for garnet–biotite

thermometry. For the latter, an average of several garnet mixing models was used as recommended (see Holdaway, 2000) assuming 3% of the iron in garnet is in the ferric state and 12% in biotite. All calculated temperatures in this study are reported to the nearest 5 °C.

Stable isotope analyses were carried out in the Department of Geology and Geophysics at the University of Wisconsin, Madison. Graphite was obtained by stirring crushed and ground rock (*c.* 30–200 cm³ of sample) in a beaker of water and removing the floating fraction. This was washed in HCl, then distilled water, dried, mixed with excess CuO and loaded into pre-fired quartz glass tubes. Evacuated tubes were fused closed and heated to 950 °C overnight. CO₂ was purified by cryogenic methods and analysed on a Finnigan MAT 251 mass spectrometer. CO₂ was extracted from whole-rock calcite by reaction in concentrated phosphoric acid at 25 °C (McCrea, 1950). ¹³C/¹²C ratios are reported in per mil using standard δ -notation relative to the PDB standard. Calcite $\delta^{13}\text{C}$ values are reproducible to better than 0.05‰ and graphite to *c.* 0.1‰. Analyses of standards over the period of data collecting were as follows: NBS-19 (calcite) $\delta^{13}\text{C} = 1.86\text{‰}$ ($n = 4$; SD = 0.01), $\delta^{18}\text{O} = 28.58\text{‰}$ ($n = 4$; SD = 0.03), UW standard calcite 93GV10 $\delta^{13}\text{C} = 2.82\text{‰}$ ($n = 7$; SD = 0.02), $\delta^{18}\text{O} = 24.19\text{‰}$ ($n = 7$; SD = 0.06), NBS-21(graphite) $\delta^{13}\text{C} = -28.33\text{‰}$ ($n = 6$; SD = 0.06) and UW graphite $\delta^{13}\text{C} = -26.51\text{‰}$ ($n = 5$; SD = 0.06). The formulation of Dunn & Valley (1992) was used to determine calcite–graphite temperatures.

RESULTS

Temperature estimates from garnet–biotite and garnet–hornblende range from 555 to 670 °C (Table 1) and those from calcite–dolomite thermometry range from 495 to 595 °C (Table 2). The spatial distribution of results from these thermometers is quite self-consistent, with temperatures ranging from *c.* 500 °C in the south to 670 °C in the north (Fig. 5).

Measured $\Delta_{\text{cal-gr}}$ values show remarkable regularity in their distribution from values $> 6.5\text{‰}$ in the south to 4.0‰ in the north (Table 3, Fig. 5). The $\Delta_{\text{cal-gr}}$ values vary systematically such that they can be contoured with only a few outliers (Fig. 5). The data are contoured again in Fig. 6, this time as isotherms based on calculated temperatures. The results show generally ENE trending isotherms of increasing temperature to the north (Fig. 6). An area of smaller $\Delta_{\text{cal-gr}}$ values indicates a localized thermal high in the vicinity of the gabbroic sheets along highway 62. Calcite–dolomite and garnet–hornblende thermometry also register this thermal high with temperatures of 575–600 °C (Fig. 5). Four kilometres east of this thermal high, two samples have unusually large $\Delta_{\text{cal-gr}}$ values (9.6‰ and 14.1‰) suggesting a localized area of lower temperatures (Fig. 6). No cation-

Table 1. Mineral compositions used for garnet–biotite thermometry (Holdaway, 2000) and garnet–hornblende thermometry (Graham & Powell, 1984).

| | BT94-1-4 | BT86-41-2 | BT86-46-4 | BT86-47-2 | CH93-1-2 | CH86-35-13 | CH86-35-15 |
|--------------------------------|----------|-----------|-----------|-----------|----------|------------|------------|
| | Garnet | | | | | | |
| SiO ₂ | 37.72 | 37.62 | 38.44 | 37.92 | 37.11 | 37.78 | 37.12 |
| TiO ₂ | na | 0.03 | na | na | 0.06 | na | 0.23 |
| Al ₂ O ₃ | 20.92 | 21.30 | 21.89 | 21.52 | 21.29 | 21.27 | 20.96 |
| MgO | 4.44 | 2.39 | 6.00 | 3.86 | 1.85 | 2.13 | 2.10 |
| CaO | 2.29 | 6.53 | 3.19 | 4.36 | 6.64 | 8.96 | 8.13 |
| MnO | 8.63 | 0.69 | 1.06 | 2.31 | 1.87 | 3.68 | 2.36 |
| FeO | 26.20 | 32.39 | 29.81 | 30.39 | 31.11 | 25.73 | 28.72 |
| Total | 100.20 | 100.95 | 100.39 | 100.36 | 99.93 | 99.55 | 99.62 |
| Si | 3.003 | 2.986 | 3.000 | 3.000 | 2.980 | 3.011 | 2.977 |
| Ti | na | 0.002 | na | na | 0.004 | na | 0.014 |
| Al | 1.963 | 1.992 | 2.013 | 2.007 | 2.015 | 1.998 | 1.981 |
| Mg | 0.527 | 0.283 | 0.698 | 0.455 | 0.222 | 0.253 | 0.251 |
| Ca | 0.196 | 0.555 | 0.267 | 0.370 | 0.571 | 0.765 | 0.698 |
| Mn | 0.582 | 0.046 | 0.070 | 0.155 | 0.127 | 0.248 | 0.160 |
| Fe | 1.745 | 2.150 | 1.945 | 2.011 | 2.089 | 1.715 | 1.926 |
| | Biotite | | | Amphibole | | | |
| SiO ₂ | 36.08 | 36.00 | 40.08 | 37.34 | 42.28 | 42.35 | 42.94 |
| TiO ₂ | 1.96 | 4.94 | 0.83 | 1.91 | 0.58 | 1.16 | 0.42 |
| Al ₂ O ₃ | 19.11 | 14.80 | 17.04 | 17.18 | 13.38 | 13.12 | 12.91 |
| Cr ₂ O ₃ | 0.03 | 0.00 | 0.01 | 0.00 | 0.00 | 0.01 | 0.07 |
| MgO | 12.62 | 10.22 | 17.99 | 14.83 | 7.16 | 9.29 | 8.44 |
| CaO | 0.02 | 0.04 | 0.12 | 0.03 | 10.97 | 10.85 | 10.87 |
| MnO | 0.20 | 0.00 | 0.01 | 0.01 | 0.03 | 0.14 | 0.26 |
| FeO | 15.56 | 20.59 | 10.85 | 15.05 | 20.71 | 17.96 | 19.08 |
| BaO | 0.13 | 0.29 | 0.03 | 0.44 | na | na | na |
| Na ₂ O | 0.20 | 0.02 | 0.34 | 0.77 | 1.51 | 1.51 | 1.88 |
| K ₂ O | 9.32 | 9.25 | 8.87 | 7.60 | 0.43 | 0.42 | 0.39 |
| H ₂ O | 4.01 | 3.93 | 4.18 | 4.05 | 1.96 | 1.98 | 1.98 |
| Total | 99.24 | 100.08 | 100.35 | 99.21 | 99.01 | 98.79 | 99.24 |
| Si | 2.697 | 2.748 | 2.902 | 2.767 | 6.457 | 6.409 | 6.502 |
| Ti | 0.110 | 0.284 | 0.045 | 0.107 | 0.067 | 0.130 | 0.048 |
| Al | 1.684 | 1.331 | 1.454 | 1.501 | 2.409 | 2.340 | 2.304 |
| Cr | 0.002 | 0.000 | 0.001 | 0.000 | 0.000 | 0.001 | 0.008 |
| Mg | 1.407 | 1.163 | 1.941 | 1.638 | 1.630 | 2.096 | 1.905 |
| Ca | 0.001 | 0.003 | 0.009 | 0.003 | 1.795 | 1.759 | 1.763 |
| Mn | 0.012 | 0.000 | 0.001 | 0.001 | 0.005 | 0.018 | 0.033 |
| Fe | 0.973 | 1.314 | 0.657 | 0.939 | 2.645 | 2.272 | 2.417 |
| Ba | 0.004 | 0.009 | 0.001 | 0.013 | na | na | na |
| Na | 0.029 | 0.003 | 0.048 | 0.110 | 0.448 | 0.443 | 0.553 |
| K | 0.889 | 0.900 | 0.819 | 0.719 | 0.083 | 0.080 | 0.076 |
| T (°C) | 670 | 585 | 555 | 570 | 565 | 600 | 585 |

BT, Bancroft topographic sheet; CH, Coe Hill; na, not analysed.

exchange thermometry is available to corroborate this.

ASSESSMENT OF THE THERMOMETRY RESULTS

The systematic variation in $\Delta_{\text{cal-gr}}$ values across the area is remarkable. This is not sufficient in itself to prove that the thermometer is accurate, but the isotopic system clearly shows self-consistent behaviour. At the southern end of the area, where temperatures are relatively low, two samples give unrealistically low temperatures, 315 and 415 °C, where other nearby samples give 520–540 °C. I presume that the graphite in these samples has not exchanged as thoroughly as that in other samples. Thus, below peak temperatures of *c.* 540 °C the reliability of the calcite–graphite thermometer is suspect. Scattering of $\Delta_{\text{cal-gr}}$ values towards unrealistically low temperatures is also seen in

Table 2. Results of calcite–dolomite thermometry (Anovitz & Essene, 1987), calcite compositions and sample assemblages.

| Sample ^a | X_{Mg} | X_{Ca} | X_{Mn} | X_{Fe} | T (°C) | Assemblage ^b |
|---------------------|----------|----------|----------|----------|----------|---|
| BT86-42-1 (11) | 0.065 | 0.933 | 0.001 | 0.001 | 580 | Qtz, Kfs, Phl, Po, Gr |
| BT86-42-2 (7) | 0.070 | 0.922 | 0.001 | 0.007 | 595 | Qtz, Olig, Phl, Tr, Di, Ttn |
| BT86-44 (4) | 0.056 | 0.942 | 0.001 | 0.001 | 550 | Qtz, Kfs, Olig, Sep, Phl, Tr, Ttn, Po, Gr |
| BT86-46-1 (6) | 0.049 | 0.925 | 0.001 | 0.025 | 545 | Qtz, Kfs, Ab, Phl, Tr, Po, Rt |
| BT86-46-2 (9) | 0.054 | 0.933 | 0.001 | 0.012 | 550 | Qtz, Kfs, Olig, Phl, Rt, Gr |
| BT96-5-2 (12) | 0.063 | 0.929 | 0.002 | 0.006 | 575 | Qtz, Olig, Phl, Tr, Di |
| BT96-5-9 (10) | 0.062 | 0.935 | 0.001 | 0.002 | 570 | Qtz, Tr, Di, Ttn, Po, Gr |
| CH86-35-14 (10) | 0.058 | 0.909 | 0.003 | 0.030 | 575 | Qtz, Olig, Tr, Ilm, Ap |
| CH86-35-19 (6) | 0.067 | 0.915 | 0.001 | 0.017 | 595 | Qtz, Olig, Phl, Chl, Tr, Ttn, Gr |
| CH86-35-23 (10) | 0.060 | 0.923 | 0.002 | 0.015 | 570 | Qtz, Olig, Ab, Phl, Tr, Rt, Po, Gr |
| CH86-71-2 (14) | 0.040 | 0.951 | 0.001 | 0.008 | 495 | Qtz, Olig, Phl, Tr |
| CH86-72-3 (24) | 0.050 | 0.944 | 0.001 | 0.005 | 530 | Qtz, Phl, Tr |
| CH93-3-1 (11) | 0.055 | 0.942 | 0.001 | 0.002 | 550 | Qtz, Pl, Phl, Tlc, Phl, Tr, Gr |
| CH96-1-3 (11) | 0.049 | 0.949 | 0.001 | 0.002 | 525 | Qtz, Olig, Phl, Tr, Gr |
| CH96-8-1 (8) | 0.047 | 0.943 | 0.001 | 0.009 | 525 | Qtz, Pl, Phl, Rt, Gr |

^aNumber of analyses averaged for each sample in parentheses.

^bAll samples contain primary calcite and dolomite; Ab, albite; Ap, apatite; Chl, chlorite; Di, diopside; Gr, graphite; Ilm, ilmenite; Kfs, K-feldspar; Olig, oligoclase; Phl, phlogopite; Pl, plagioclase; Po, pyrrhotite; Py, pyrite; Qtz, quartz; Rt, rutile; Sep, scapolite; Tlc, talc; Ttn, titanite; Tr, tremolite; Tur, tourmaline.

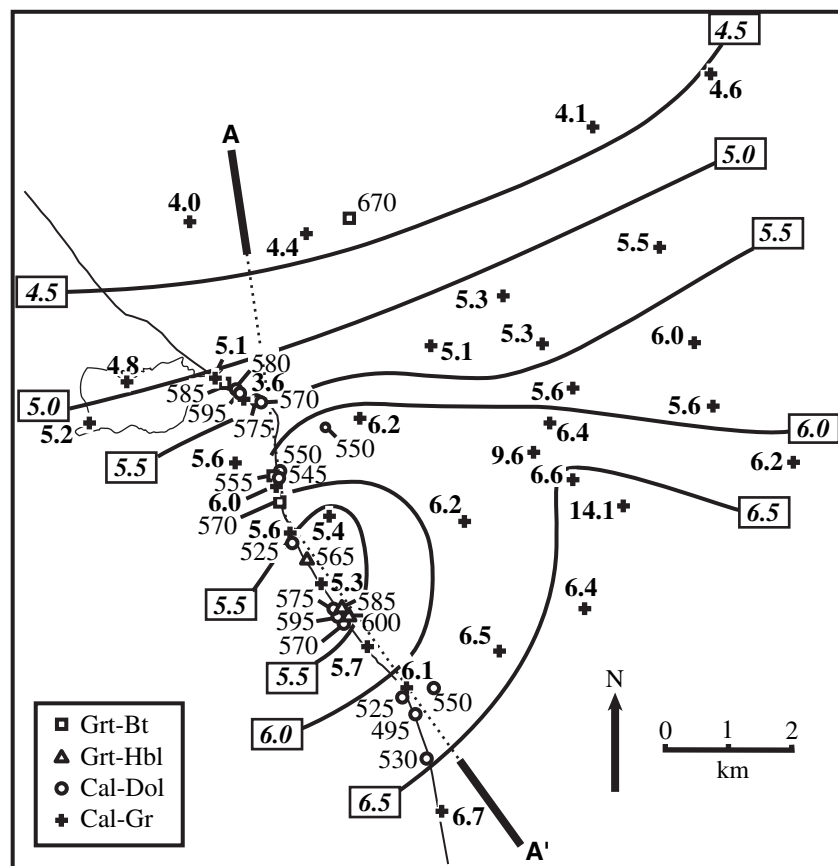


Fig. 5. Temperatures determined from calcite–dolomite, garnet–biotite and garnet–hornblende thermometry and $\Delta_{\text{cal-gr}}$ values contoured at 0.5% intervals.

low-grade marbles (*c.* 500 °C) just to the north of Madoc (Dunn & Valley, 1992), and in occasional samples throughout this terrane (Fig. 2; Rathmell *et al.*, 1999).

One notable outlier is sample BT86-42-1, the dolomite-rich marble mentioned earlier with unusual late-stage textures near L'Amable Lake. This sample has an abnormally small $\Delta_{\text{cal-gr}}$ value (3.6‰) that corresponds with an anomalously high temperature of 700 °C. Five

independent temperature determinations for samples within a few hundred metres of BT86-42-1 give 570–595 °C, four from calcite–dolomite thermometry and one from garnet–biotite (Fig. 5). The unusually high-temperature fractionation indicated by this sample is important because it cannot be explained by incomplete isotopic exchange. Dunn & Valley (1992) showed that calcite–graphite pairs exposed to temperatures above 500 °C in a contact aureole are not reset during

Table 3. Isotopic composition of calcite and graphite, Cal–Gr thermometry results and sample descriptions.

| | $\delta^{18}\text{O}_{\text{cal}}$ | $\delta^{13}\text{C}_{\text{cal}}$ | $\delta^{13}\text{C}_{\text{gr}}$ | $\Delta_{\text{cal-gr}}$ | T (°C) ^a | Independent T (°C) ^b | Grain size ^c (μm) | | % Calcite | % Dolomite | Assemblage ^d |
|-----------|------------------------------------|------------------------------------|-----------------------------------|--------------------------|-----------------------|-----------------------------------|---|----------|-----------|------------|----------------------------|
| | | | | | | | Graphite | Calcite | | | |
| BT86-42-1 | 21.72 | 0.59 | -2.96 | 3.55 | 700 | 580 | 50 | 100–600 | 33 | 33 | Qtz, Kfs, Phl, Po |
| BT93-4-3 | 23.42 | 0.66 | -3.76 | 4.42 | 635 | 660 | 400 | 600–3000 | 97 | 0 | Qtz, Pl, Phl, Po |
| BT93-10 | 23.56 | 1.18 | -4.45 | 5.63 | 565 | 550 | 40 | 300–1600 | 83 | 3 | Qtz, Kfs, Phl, Rt |
| BT94-3-10 | 22.85 | 0.56 | -4.56 | 5.12 | 595 | 590 | 70 | 500–3000 | 60 | 5 | Scp, Phl, Tr, Di |
| BT94-47-1 | 21.07 | 2.94 | -3.24 | 6.18 | 540 | 555 | 30 | 80–400 | 65 | 15 | Qtz, Pl, Phl, Chl, Ttn, Rt |
| BT94-50-2 | 19.97 | 2.13 | -3.15 | 5.28 | 585 | | 70 | 200–800 | 66 | 0 | Qtz, Pl, Kfs, Phl, Di, Ttn |
| BT94-52 | 21.37 | 3.50 | -1.84 | 5.34 | 580 | | 60 | 250–800 | 80 | 5 | Pl, Phl, Chl, Tr |
| BT94-59-1 | 19.36 | 4.82 | -1.34 | 6.16 | 540 | | 35 | 200–800 | 80 | 3 | Qtz, Pl, Phl, Chl |
| BT94-62-2 | 20.65 | -2.00 | -5.98 | 3.98 | 665 | 680 | 300 | 100–700 | 85 | 5 | Phl, Tr, Po, Ttn |
| BT95-7 | 23.19 | 2.30 | -2.89 | 5.19 | 590 | 580 | 80 | 400–2000 | 90 | 0 | Qtz, Pl, Rt |
| BT95-8 | 22.73 | 0.33 | -4.47 | 4.80 | 610 | 600 | 800 | 100–1200 | 56 | 0 | Qtz, Phl, Di, Rt, Ttn |
| BT95-26-1 | 21.17 | 3.17 | -1.92 | 5.09 | 595 | | 100 | 300–3000 | 93 | 2 | Qtz, Pl, Phl |
| BT95-30-2 | 20.60 | 2.98 | -1.65 | 4.63 | 625 | | 120 | 200–1500 | 68 | 8 | Pl, Phl, Ttn |
| BT95-37-2 | 17.87 | -2.24 | -6.38 | 4.14 | 655 | | 500 | 400–2500 | 60 | 0 | Phl, Di, Tur, Py |
| BT95-39-1 | 19.01 | 2.58 | -2.87 | 5.45 | 575 | | 60 | 400–1400 | 78 | 0 | Qtz, Phl, Tur |
| BT95-47 | 19.81 | 1.43 | -4.74 | 6.17 | 540 | | 60 | 200–1400 | 95 | 2 | Chl |
| BT95-52-1 | 22.38 | 3.70 | -1.89 | 5.59 | 570 | | 70 | 200–1400 | 93 | 2 | Phl, Tlc |
| BT95-55-2 | 17.63 | 5.20 | -0.81 | 6.01 | 550 | | 50 | 100–500 | 70 | 0 | Qtz, Pl, Kfs, Phl, Rt |
| BT95-57-1 | 21.80 | 3.08 | -2.89 | 5.97 | 550 | 550 | 50 | 100–800 | 96 | 2 | Pl, Phl, Qtz |
| BT95-60-1 | 18.95 | 4.24 | -1.11 | 5.35 | 580 | 560 | 50 | 300–1000 | 83 | 0 | Qtz, Pl, Phl |
| BT95-63 | 18.46 | 4.07 | -2.51 | 6.58 | 520 | | 70 | 100–600 | 38 | 0 | Qtz, Kfs, Tr, Ttn |
| BT95-65 | 23.44 | 2.96 | -11.10 | 14.06 | 315 | | 40 | 300–1200 | 81 | 0 | Qtz, Pl, Phl, Py |
| BT95-70-2 | 17.02 | 4.01 | -5.63 | 9.64 | 415 | | 50 | 100–600 | 90 | 0 | Qtz, Pl, Phl, Rt |
| BT95-71-1 | 16.54 | 4.62 | -1.82 | 6.44 | 530 | | 60 | 80–400 | 83 | 0 | Qtz, Kfs, Phl |
| BT95-72-2 | 16.68 | 4.57 | -1.01 | 5.58 | 570 | | 70 | 200–600 | 85 | 0 | Qtz, Pl, Phl, Tur, Ttn |
| CH93-6-1 | 22.26 | 3.22 | -3.32 | 6.54 | 525 | 545 | 100 | 600–2400 | 80 | 10 | Qtz, Phl, Tr, Rt |
| CH95-14 | 17.32 | 5.05 | -1.38 | 6.43 | 530 | | 20 | 60–500 | 74 | 0 | Qtz, Phl, Tr, Ttn |
| CH96-1-2 | 21.30 | 6.17 | 0.10 | 6.07 | 545 | 550 | 50 | 300–1200 | 88 | 0 | Qtz, Phl, Tr |
| CH96-4-2 | 19.46 | 3.98 | -1.70 | 5.68 | 565 | 580 | 70 | 400–1600 | 95 | 0 | Pl, Phl |
| CH96-6-1 | 19.53 | 5.94 | 0.69 | 5.25 | 585 | 585 | 100 | 600–2400 | 95 | 0 | Qtz, Pl, Phl, Chl |
| CH96-8-1 | 19.67 | 4.56 | -0.99 | 5.55 | 570 | 570 | 40 | 300–1600 | 95 | 2 | Qtz, Pl, Phl, Rt |
| UM94-7-2 | 19.89 | 2.32 | -4.42 | 6.74 | 515 | 500 | 70 | 80–500 | 82 | 0 | Qtz, Pl, Phl, Tr, Rt |

^aTemperature (rounded to the nearest 5 °C) from formulation of Dunn & Valley (1992), $\Delta_{\text{cal-gr}} = 5.81 \times 10^6 T^{-2}$ (K) – 2.61.

^bTemperature assigned from nearby cation-exchange thermometry (Fig. 7, see text).

^cFor graphite flakes, this is the representative upper limit determined by reflected light microscopy; for calcite, the representative range is given.

^dIn addition to calcite, graphite and \pm dolomite, Chl, chlorite; Di, diopside; Kfs, K-feldspar; Phl, phlogopite; Pl, plagioclase; Po, pyrrhotite; Py, pyrite; Qtz, quartz; Rt, rutile; Scp, scapolite; Tlc, talc; Ttn, titanite; Tr, tremolite; Tur, tourmaline.

regional metamorphism at 500 °C. Thus, assuming that graphite is more difficult to recrystallize than calcite, and because the calcite in this sample shows late-stage crystallization, the likeliest explanation for this anomalous $\Delta_{\text{cal-gr}}$ value is modification of the calcite $\delta^{13}\text{C}$ after the peak of metamorphism. Samples showing complex carbonate textures or low percentage of calcite relative to graphite should be avoided for calcite–graphite thermometry.

Temperatures determined by calcite–graphite are directly compared with cation-exchange thermometry (calcite–dolomite, garnet–biotite and garnet–hornblende) along a traverse that closely follows highway 62 (A–A' in Fig. 5). Temperatures determined by cation-exchange thermometry were projected onto this traverse and a smooth curve fit by hand to the results (dashed line in Fig. 7). Where multiple samples indicate a range of temperatures, somewhat greater credence is given to higher temperatures than to lower temperatures in order to allow for retrograde effects. Calcite–graphite data are then projected onto this curve for samples that lie within *c.* 2 km of the traverse, and an 'independent temperature' from cation-exchange thermometry is assigned to each (see Table 3). Two calcite–dolomite sample temperatures

fall *c.* 50 °C below this line, consistent with the findings of Rathmell *et al.* (1999). Sample BT86-42-1 is excluded from this comparison.

Calcite–graphite temperatures from the Dunn & Valley (1992) empirical calibration agree quite well with temperatures determined by the cation-exchange thermometers (Fig. 8). The calibration of Wada & Suzuki (1983) is not shown, but is within 8 °C of Dunn & Valley for their overlapping temperature range, however Wada & Suzuki's calibration covers a smaller range. The empirical calibration of Morikiyo (1984) also agrees very well overall, but the fit is less good outside the range 550–600 °C. The theoretical calibration of Chacko *et al.* (1991) shows excellent agreement at 600 °C and higher, but the fit is poor below 600 °C. The theoretical calibration of Polyakov & Kharlashina (1995), adjusted for 500 MPa pressure, does not fit the data well (Fig. 8). The empirical thermometer of Kitchen & Valley (1995) is not compared as most of the data in this study are outside the temperature range of their calibration, but their formulation gives results similar to that of Chacko *et al.* (1991).

Repeated analyses of standards gave an analytical uncertainty in the $\delta^{13}\text{C}$ measurements of $\pm 0.04\%$ (2 sd) for calcite and $\pm 0.12\%$ (2 sd) for graphite. Sample

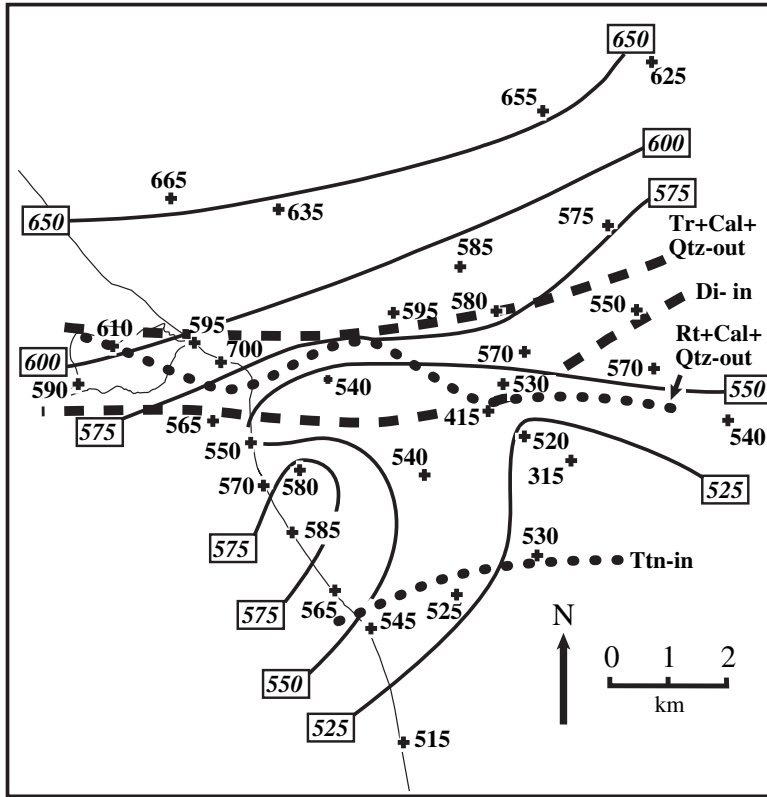


Fig. 6. Mineral reaction isograds from Fig. 4 superimposed on the contoured results of the calcite-graphite thermometry (rounded to the nearest 5 °C).

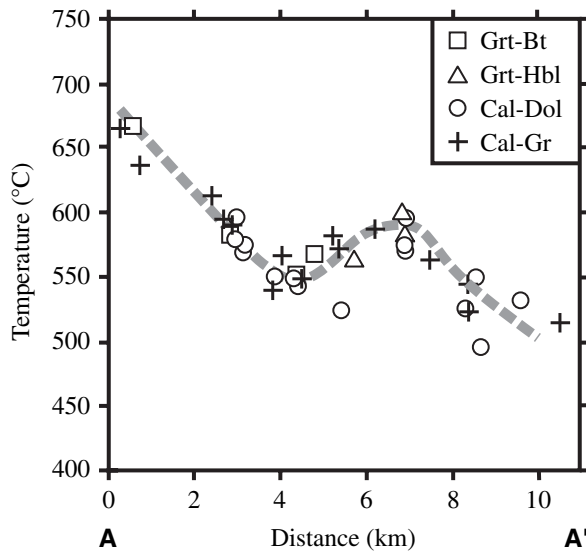


Fig. 7. Results of the cation-exchange thermometry, and calcite-graphite thermometry projected onto traverse A-A' of Fig. 5. The dashed curve is fit to the cation-exchange thermometry results and used to assign independent temperature estimates for calcite-graphite samples.

duplicates have equivalent uncertainties. An uncertainty of $\pm 0.20\%$ in the $\Delta_{\text{cal-gr}}$ value corresponds to an uncertainty of less than ± 15 °C (for temperatures below 670 °C), which is, therefore, the minimum relative uncertainty in precision possible in this study.

Assumptions regarding equilibrium and calibration render the absolute accuracy significantly larger, but unconstrained.

TEMPERATURE CONSTRAINTS FROM MARBLE MINERAL EQUILIBRIA

Only calcite-rich marble samples were considered in delineating the isograds in Fig. 4. In particular, I excluded 'feather amphibolite' samples, a calcite-bearing lithology widespread throughout the region. These para-amphibolite rocks are named for their curved splays of amphibole and represent a protolith of marl or influx of abundant volcanic ash into the carbonate facies sedimentary basin. Their calcite content varies and they generally comprise abundant plagioclase and aluminous hornblende, \pm quartz, \pm garnet. Titanite is ubiquitous in these para-amphibolites and clinopyroxene growth appears to be inhibited in some samples and advanced in others such that inclusion of this rock type in the isograd maps would expand the titanite stability field to cover the entire area and greatly complicate the diopside and tremolite + calcite + quartz fields. By excluding para-amphibolite and similar calc-silicate rocks, the isograd maps represent a narrower range of bulk composition.

The $T-X(\text{CO}_2)$ relations in marble independently support the thermometry results. The diopside-in and tremolite + calcite + quartz-out isograds correspond to *c.* 550–575 and 575–600 °C respectively (Fig. 6).

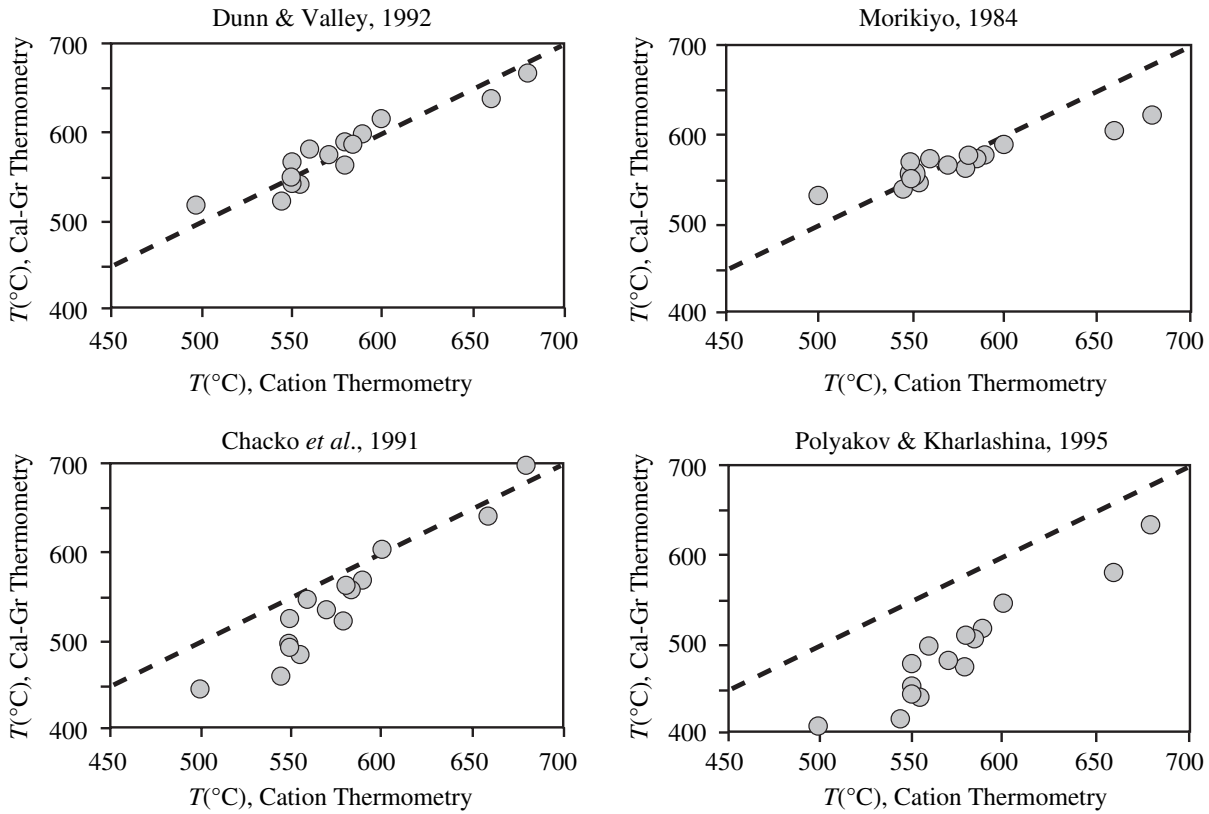


Fig. 8. Comparison of calcite–graphite thermometry to cation-exchange thermometry for samples along traverse A–A'. The dashed lines represent one-to-one correspondence. Dunn & Valley (1992) provides the best fit over the full data range.

The titanite-in isograd crosses the 525 and 550 °C isotherms and the rutile + calcite + quartz-out isograd crosses the 550–600 °C isotherms. Mineral compositions vary and as a result show a range of $T-X(\text{CO}_2)$ relations (Dunn *et al.*, 1995). $T-X(\text{CO}_2)$ relations in the $\text{K}_2\text{O}-\text{CaO}-\text{MgO}-\text{Al}_2\text{O}_3-\text{SiO}_2-\text{CO}_2-\text{H}_2\text{O}$ system are shown in Fig. 9 for two representative marble samples with restrictive assemblages, as derived from the GEØ-CALC program of Berman & Perkins (1987) and database of Berman (1988). Sample BT86-42-2 contains the invariant assemblage $\text{Tr} + \text{Cal} + \text{Qtz} + \text{Di} + \text{Dol}$ (+Phl + Pl + Ttn), and sample BT94-53-1 contains the univariant assemblage, $\text{Tr} + \text{Cal} + \text{Qtz} + \text{Di}$ (+Phl + Pl). Phase relations in Fig. 9 have been adjusted for solid solutions using mixing-on-sites activity models, $\alpha_{\text{Di}} = X_{\text{Ca}}X_{\text{Mg}}$, $\alpha_{\text{Tr}} = X_{\text{Ca}}^2X_{\text{Mg}}^5X_{\text{OH}}^2$, $\alpha_{\text{Phl}} = X_{\text{K}}X_{\text{Mg}}^3X_{\text{OH}}^2$, and other minerals assumed pure. Iron–magnesium substitution is one of the principal causes of deviation from end-member compositions. BT86-42-2 is a relatively low-iron marble ($\alpha_{\text{Di}} = 0.90$, $\alpha_{\text{Tr}} = 0.59$, $\alpha_{\text{Phl}} = 0.50$) and BT94-53-1 is slightly more iron-rich ($\alpha_{\text{Di}} = 0.72$, $\alpha_{\text{Tr}} = 0.19$, $\alpha_{\text{Phl}} = 0.20$). Metamorphic pressure estimated from garnet–aluminosilicate–quartz–plagioclase (GASP) barometry following Holdaway (2000) is 530 MPa at 670 °C (sample BT94-1-4 near the

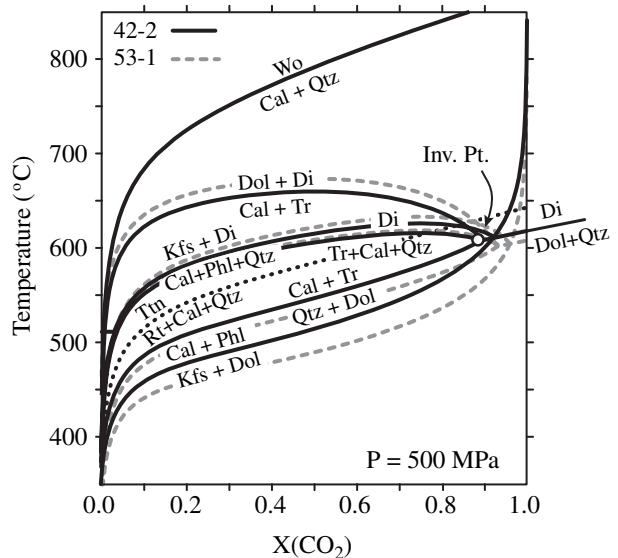


Fig. 9. Temperature– $X(\text{CO}_2)$ diagram adjusted for mineral solid solutions in typical marble samples (see text for details). For clarity, only the reaction curves for 42-2 are labelled. Sample 42-2 lies at the invariant point indicated. Sample 53-1 lies on the tremolite + calcite + quartz = diopside reaction curve. The rutile + calcite + quartz = titanite reaction (dotted) is shown for end-member compositions.

northern edge of area, garnet composition in Table 1, plagioclase = An₄₅). Rathmell *et al.* (1999) reported GASP pressures of 500–550 MPa for this same location; 500 MPa is used for calculating T - $X(\text{CO}_2)$ relations in Fig. 9.

The invariant point appropriate for BT86-42-2 is at 610 °C, $X(\text{CO}_2) = 0.90$. This sample locality lies between the 575 and 600 °C isotherms, and thus the calcite–graphite thermometry agrees well with the mineral equilibria, within *c.* 25 °C. This sample also contains titanite and the locality is above the rutile + calcite + quartz-out isograd, yet the calculated invariant point is within the rutile + calcite + quartz stability field. Only the end-member reaction is shown in Fig. 9, but presumably solid solution effects increase the titanite stability field to temperatures below 600 °C at this location; titanite compositions have not been determined.

An isograd based on diopside-in or tremolite + calcite + quartz-out cannot be tightly constrained because, for water-rich fluid conditions, the reaction can occur at a wide range of temperatures (Fig. 9). However, if regional metamorphic fluid compositions were generally CO₂-rich, as suggested for sample BT86-42-2, then the diopside-in isograd would be expected around 575–600 °C and the tremolite + calcite + quartz-out isograd should occur no higher than *c.* 620 °C. These temperatures are only 25 °C or so higher than the results of the calcite–graphite thermometry, which is reasonably good agreement. If the metamorphic pressure was 100 MPa lower, still within the uncertainty in the GASP barometry, then these reaction isograds would lie 30 °C lower in temperature and agreement with the thermometry would be excellent.

The isotherms and the mineral isograds all indicate that temperature increased northward, but the connection of these features to one another in detail remains unclear. For example, the diopside-in isograd generally lies between the 525 and 575 °C isotherms, however, diopside is not found within the localized thermal high in the southern part of the area, even though temperatures there exceeded 575 °C. Deviations between isotherms and isograds may result from variations in rock composition, metamorphic fluid composition, the timing of heating and deformation (including polymetamorphism), or combinations of these. Many workers have shown that mineral reactions involving fluids can proceed at different temperatures as a result of different fluid infiltration histories among samples and localities (e.g. see Ferry, 1991, and references therein). In the absence of infiltrating fluid, the diopside-forming reaction will produce CO₂-rich fluid and proceed at relatively high temperature (closed-system behaviour – although fluid is expelled). Infiltration of H₂O-rich fluid will drive the diopside-forming reaction at a lower temperature (open-system behaviour).

It may reasonably be assumed that marble compositions are uniform throughout the area, and if it is further assumed that all rocks in the area experienced a similar metamorphic history, then the absence of diopside in the localized thermal high requires locally variable fluid behaviour during metamorphism. It follows that the samples, which define the diopside-in isograd across the area experienced open-system fluid behaviour and the diopside was stabilized at lower temperature by more H₂O-rich conditions, especially in the central and eastern part of the area where diopside was stable at lower temperatures. The area of localized thermal high without diopside attained more CO₂-rich fluid conditions, presumably from internal buffering, and thus diopside formation was inhibited in those rocks. Similarly, the tremolite + calcite + quartz-out isograd occurs at lower temperatures in the central and eastern part of the area, *c.* 575 °C, and at higher temperature to the west, *c.* 600 °C. The tremolite + calcite + quartz assemblage is stabilized to higher temperature by buffered fluid conditions [thermal maximum at $X(\text{CO}_2) = 0.75$], therefore, the apparent E–W thermal contrast of this isograd may indicate relatively more closed-system behaviour in marble to the west near L'Amable Lake. More work is needed to address these issues, but it appears that fluid compositions in this marble belt varied systematically on the scale of kilometres during metamorphism.

DISCUSSION

The results demonstrate a gradual temperature increase northward (i.e. 'field gradient') in the study area that averages *c.* 15 °C km⁻¹ (150 °C over 10 km), but is closer to 30 °C km⁻¹ in the northern half of the area. The ENE trend of the isotherms in this area roughly parallels that of mineral isograds (Fig. 6). The ENE trending isotherms also agree with regional isograds of Carmichael *et al.* (1978) and regional isotherms of Rathmell *et al.* (1999).

Several studies have shown that the calcite–dolomite solvus system tends to partially reset upon cooling from temperatures over 600 °C (e.g. Essene, 1989). Similarly, Rathmell *et al.* (1999) concluded that the garnet–biotite and calcite–graphite systems show good agreement across this terrane, but the calcite–dolomite system appears to show resetting of 50–100 °C in the higher grade parts of the region (e.g. their 550 °C calcite–dolomite isotherm nearly coincides with their 600 °C calcite–graphite isotherm). In the present study, two samples yield calcite–dolomite solvus temperatures that are 50 °C too low compared with nearby samples (Fig. 7), consistent with the findings of Rathmell *et al.* (1999), otherwise the calcite–dolomite and calcite–graphite thermometers show excellent agreement over the 500–600 °C range. I have not applied calcite–dolomite thermometry in the part of this area that exceeded 600 °C.

This study does not directly address the question of whether or not the temperature– $\Delta_{\text{cal-gr}}$ relations observed in rocks metamorphosed below *c.* 600 °C represent the *equilibrium* isotopic exchange between calcite and graphite. The data obtained in this study show exceptionally regular variation across the study area and agree well with cation-exchange systems. If the equilibrium $\Delta_{\text{cal-gr}}$ values are considerably smaller than those observed, as suggested by Chacko *et al.* (1991) and supported by the agreement of empirical and theoretical calibrations at 650–850 °C, then one might expect greater sample to sample variation in C-isotope exchange. The smooth variation in $\Delta_{\text{cal-gr}}$ values observed suggests a well-behaved system, whether recording equilibrium fractionations or not.

The calcite–graphite isotopic system has shown consistent behaviour below 650 °C in regional metamorphic terranes (Morikiyo, 1984; Rathmell *et al.*, 1999; this study) as well as in contact aureoles. Wada & Suzuki (1983) studied this system in a contact aureole, and, as noted earlier, their calibration fits regional metamorphic data in this study very well. Similarly, Okuyama-Kusunose *et al.* (2003) found smooth variation in $\Delta_{\text{cal-gr}}$ values in three different contact aureoles, and, although they do not have independent thermometry, they concluded that carbon isotopes had in fact equilibrated at temperatures in the range 560–595 °C, using the calibrations of Kitchen & Valley (1995) and Polyakov & Kharlashina (1995). [The Dunn & Valley (1992) calibration on their rocks yields 595–620 °C.] Thus, rocks with very different thermal histories appear to have equivalent variation in calcite–graphite carbon isotope fractionations with temperature, which is remarkable if this is a non-equilibrium system. In any case, this study shows that the calcite–graphite thermometer is capable of producing self-consistent and reliable temperatures in amphibolite facies marble. Limited data available in this study suggests that the thermometer becomes irregular at temperatures below *c.* 540 °C.

Sampling density in the Rathmell *et al.* (1999) study was considerably less than that of this study, therefore, the position of their regional isograds within the area of this study relied on interpolating between more widely separated data points. The 650 °C isotherm in this study, essentially coincides with that of Rathmell *et al.*, however, their 550 °C isotherm is placed 20 km to the south of the area of this study. Thus, the Rathmell *et al.* results indicate a regional metamorphic field gradient of *c.* 5 °C km⁻¹, rather than the 30 °C km⁻¹ (locally) indicated by this study. The regional isotherms of Rathmell *et al.* (1999) based upon garnet–biotite and calcite–dolomite thermometry indicate even smaller field gradients and are further from agreement with the results of this study.

Field gradients in regional metamorphic settings are highly variable. For example, peak metamorphic temperatures in the Adirondack Mountain Lowlands, New York, vary <25 °C over 40 km (<1 °C km⁻¹),

whereas in the Central Adirondack Highlands gradients appear to be more typically 2–3 °C km⁻¹ (Kitchen & Valley, 1995). In contrast, thermal contact aureoles typically show gradients of 100–200 °C km⁻¹. In both regional and contact metamorphic settings, faulting or deformation during and after peak thermal events may obscure the original temperature relations, but it is clear from this study that systematic temperature gradients are not likely to be recognized by large-scale sampling methods and care must be taken when drawing local conclusions from regional data.

The thermal gradient documented in this study is consistent with large-scale tectonic perspectives. The age of metamorphism is *c.* 1060–1020 Ma based on U/Pb dating of titanite in the northern Elzevir and adjacent Bancroft terranes (Mezger *et al.*, 1993). The boundary between these terranes is the extensional Bancroft shear zone and titanite ages within the shear zone (1046–1032 Ma) are in the same range as those on either side. Hornblende ⁴⁰Ar/³⁹Ar cooling ages differ across the Bancroft shear zone and suggest fairly rapid uplift and cooling of the Elzevir terrane (van der Pluijm *et al.*, 1994).

The heat source and timing of metamorphism in the thermal high south of L'Amable Lake associated with metagabbroic rocks remains unclear. It is tempting to call upon the gabbroic rocks as the heat source, but these are themselves metamorphosed to garnet assemblages that yield garnet–hornblende temperatures equal to nearby calcite–dolomite and calcite–graphite temperatures. These rocks are similar to the large *c.* 1240 Ma gabbroic plutons in the Elzevir terrane (biotite-bearing gabbro with dark purplish plagioclase in hand sample), and may be of the same age. Their conversion to garnet amphibolite most likely occurred during the 1060–1020 Ma Ottawan orogeny, in which case the locally elevated temperature must be attributed to causes other than contact metamorphism.

CONCLUSIONS

The calcite–graphite isotopic system provides useful thermometry in amphibolite facies marble, revealing orderly variation in $\Delta_{\text{cal-gr}}$ values across the study area that corresponds to temperatures from below 525 °C in the south to over 650 °C in the north. These results agree very well with garnet–biotite, garnet–hornblende and calcite–dolomite cation-exchange thermometry. Mineral isograds in marble based on the reactions tremolite + calcite + quartz = diopside and rutile + calcite + quartz = titanite, are roughly parallel with calcite–graphite isotherms. *T*–*X*(CO₂) relations for these isograds and for marble samples adjusted for mineral solid solutions are in good agreement with the thermometry results. Deviations between mineral isograds and the local isotherms are best explained by differences in metamorphic fluid composition.

Despite the success in applying the calcite–graphite thermometer to amphibolite facies marble in this study, it is likely that the system does not represent equilibrium isotopic exchange below *c.* 650 °C. No data are currently available to explain why the isotopic system behaves so predictably in these rocks. I suggest that, at present, the calibration of Dunn & Valley (1992) yields the best results between *c.* 525 and 650 °C, however, scatter towards low, unreliable temperatures becomes a problem below *c.* 540 °C. At temperatures above 650 °C, the Kitchen & Valley (1995) empirical calibration agrees well with available theoretical calibrations.

ACKNOWLEDGEMENTS

I am deeply grateful to J. Valley for access to his laboratories, many insightful discussions and insightful reviews. I thank M. Spicuzza for guidance in the UW isotope laboratory and M. Jercinovic for guidance in the UMass microprobe laboratory. M. Holdaway kindly provided computer algorithms for mineral activity and *P–T* calculations. G. Marchand produced many excellent polished thin sections. Mount Holyoke students who assisted with field work and other activities related to this project over many years include C. G. Baker, E. Banks, E. Dopfel, G. Elliott, S. Principato, S. Stone, H. Waterman and V. Wyser-Pratt. Thoughtful reviews by A. Barth, J. R. O’Neil and M. Satish-Kumar improved the manuscript. Funding is gratefully acknowledged from NSF (EAR9305104 and 0126661).

REFERENCES

- Anovitz, L. M. & Essene, E. J., 1987. Phase equilibria in the system $\text{CaCO}_3\text{--MgCO}_3\text{--FeCO}_3$. *Journal of Petrology*, **28**, 389–414.
- Anovitz, L. M. & Essene, E. J., 1990. Thermobarometry and pressure–temperature paths in the Grenville Province of Ontario. *Journal of Petrology*, **31**, 197–241.
- Arita, Y. & Wada, H., 1990. Stable isotopic evidence for migration of metamorphic fluids along grain boundaries of marble. *Geochemical Journal*, **24**, 173–186.
- Bergfeld, D., Nabelek, P. I. & Labotka, T. C., 1996. Carbon isotope exchange during polymetamorphism in the Panamint Mountains, California, USA. *Journal of Metamorphic Geology*, **14**, 199–212.
- Berman, R. G., 1988. Internally consistent thermodynamic data for minerals in the system $\text{Na}_2\text{O--K}_2\text{O--CaO--MgO--FeO--Fe}_2\text{O}_3\text{--SiO}_2\text{--TiO}_2\text{--H}_2\text{O--CO}_2$. *Journal of Petrology*, **29**, 445–522.
- Berman, R. G. & Perkins, E. H., 1987. GEØ-CALC: software for calculation and display of pressure–temperature–composition phase diagrams. *American Mineralogist*, **72**, 861–862.
- Bottinga, Y., 1969. Calculated fractionation factors for carbon and hydrogen isotope exchange in the system calcite–carbon dioxide–graphite–methane–hydrogen–water vapor. *Geochimica et Cosmochimica Acta*, **33**, 49–64.
- Brady, J. B., 1995. Diffusion data for silicate minerals, glasses, and liquids. In: *Mineral Physics and Crystallography: a Handbook of Physical Constants* (ed. Ahrens, T. H.) *Reference Shelf 2*, pp. 269–290. American Geophysical Union, Washington, DC.
- Buseck, P. R. & Huang, B. J., 1985. Conversion of carbonaceous material to graphite during metamorphism. *Geochimica et Cosmochimica Acta*, **49**, 2003–2016.
- Carmichael, D. M., Moore, J. M. & Skippen, G. B., 1978. Isograds around the Hastings metamorphic ‘low’. In: *Toronto ‘78 Field Trips Guidebook* (eds Currie, A. L. & Mackasey, W. O.), pp. 325–346. Geological Association of Canada, Toronto, Canada.
- Carr, S. D., Easton, R. M., Jamieson, R. A. & Culshaw, N. G., 2000. Geologic transect across the Grenville orogen of Ontario and New York. *Canadian Journal of Earth Sciences*, **37**, 193–216.
- Chacko, T., Mayeda, T. K., Clayton, R. N. & Goldsmith, J. R., 1991. Oxygen and carbon isotope fractionations between CO_2 and calcite. *Geochimica et Cosmochimica Acta*, **55**, 2867–2882.
- Cosca, M. A., Essene, E. J., Kunk, M. J. & Sutter, J. F., 1992. Differential unroofing within the Central Metasedimentary Belt of the Grenville Orogen: constraints from $^{40}\text{Ar}/^{39}\text{Ar}$ thermometry. *Contributions to Mineralogy and Petrology*, **110**, 211–225.
- Dodson, M. H., 1973. Closure temperature in cooling geochronological and petrological systems. *Contributions to Mineralogy and Petrology*, **40**, 259–274.
- Dunn, S. R. & Valley, J. W., 1992. Calcite–graphite isotope thermometry: a test for polymetamorphism in marble, Tudor gabbro aureole, Ontario, Canada. *Journal of Metamorphic Geology*, **10**, 487–501.
- Dunn, S. R. & Valley, J. W., 1996. Polymetamorphic fluid–rock interaction of the Tudor gabbro and adjacent marble, Ontario. *American Journal of Science*, **296**, 244–295.
- Dunn, S. R. & Stone, S. B. & Wyser-Pratte, V. L., 1995. Mineral equilibria in amphibolite facies marble, S. Ontario and implications for *T–X*(CO_2) relations. *Geological Society of America, Abstracts with Programs*, **27**, 317.
- Easton, R. M., 2000. Metamorphism of the Canadian shield, Ontario, Canada. II. Proterozoic metamorphic history. *Canadian Mineralogist*, **38**, 319–344.
- Eiler, J. M., Baumgartner, L. P. & Valley, J. W., 1992. Inter-crystalline stable isotope diffusion: a fast grain boundary model. *Contributions to Mineralogy and Petrology*, **112**, 543–557.
- Essene, E. J., 1989. The current status of thermobarometry in metamorphic rocks. In: *Evolution of Metamorphic Belts, Special Publication 43* (eds Daly, J. S., Cliff, R. A. & Yardley, B. W. D.), pp. 1–44. Geological Society, London.
- Farquhar, J., Chacko, T. & Frost, B. R., 1993. Strategies for high-temperature oxygen isotope thermometry: a worked example from the Laramie Anorthosite Complex, Wyoming, USA. *Earth and Planetary Science Letters*, **117**, 407–422.
- Farquhar, J., Hauri, E. & Wang, J. H., 1999. New insights into carbon fluid chemistry and graphite precipitation: SIMS analysis of granulite facies graphite from Ponnudi, South India. *Earth and Planetary Science Letters*, **171**, 607–621.
- Ferry, J. M., 1991. Dehydration and decarbonation reactions as a record of fluid infiltration. In: *Contact Metamorphism* (ed. Kerrick, D. M.), *Reviews in Mineralogy*, **26**, 351–393. Mineralogical Society of America, Washington DC.
- Giletti, B. J., 1986. Diffusion effects on oxygen isotope temperature of slowly cooled igneous and metamorphic rocks. *Earth and Planetary Science Letters*, **77**, 218–228.
- Graham, C. M. & Powell, R., 1984. A garnet–hornblende geothermometer: calibration, testing, and application to the Pelona Schist, southern California. *Journal of Metamorphic Geology*, **2**, 13–31.
- Hewitt, D. F., 1957. *Geology of Cardiff and Faraday Townships*, Map no. 1957-1. Ontario Department of Mines, Ontario.
- Hewitt, D. F. & James, W., 1955. *Geology of Dungannon and Mayo Townships*, Map no. 1955-8. Ontario Department of Mines, Ontario.
- Holdaway, M. J., 2000. Application of new experimental and garnet Margules data to the garnet–biotite geothermometer. *American Mineralogist*, **85**, 881–892.

- Kitchen, N. E. & Valley, J. W., 1995. Carbon isotope thermometry in marbles of the Adirondack Mountains, New York. *Journal of Metamorphic Geology*, **13**, 577–594.
- Kohn, M. J. & Spear, F. S., 1991. Error propagation for barometers 2: application to rocks. *American Mineralogist*, **76**, 138–147.
- Labotka, T. C., Cole, D. R., Riciputi, L. R. & Fayek, M., 2004. Diffusion of C and O in calcite from 0.1 to 200 MPa. *American Mineralogist*, **89**, 799–806.
- Lumbers, S. B., 1969. *Geology of Limerick and Tudor Townships, Hastings County. Geological Report*, **67**, 110. Ontario Department of Mines, Ontario.
- McCrea, J. M., 1950. On the isotope chemistry of carbonates and a paleotemperature scale. *Journal of Chemical Physics*, **18**, 849–857.
- Mezger, K., Essene, E. J., van der Pluijm, B. A. & Halliday, A. N., 1993. U–Pb geochronology of the Grenville orogeny of Ontario and New York: constraints on ancient crustal tectonics. *Contributions to Mineralogy and Petrology*, **114**, 13–26.
- Moecher, D. P., Valley, J. W. & Essene, E. J., 1994. Extraction and stable isotope analysis of CO₂ from scapolite in deep crustal granulites and xenoliths. *Geochimica et Cosmochimica Acta*, **58**, 959–967.
- Moore, J. M. & Thompson, P. H., 1980. The Flinton Group: a late Precambrian metasedimentary succession in the Grenville Province of eastern Ontario. *Canadian Journal of Earth Sciences*, **17**, 1685–1707.
- Morikiyo, T., 1984. Carbon isotopic study on coexisting calcite–graphite in the Ryoike metamorphic rocks, northern Kiso district, central Japan. *Contributions to Mineralogy and Petrology*, **87**, 251–259.
- Morrison, J. & Barth, A. P., 1993. Empirical tests of carbon isotope thermometry in granulites from southern California. *Journal of Metamorphic Geology*, **11**, 789–800.
- Okuyama-Kusunose, Y., Morikiyo, M., Kawabata, A. & Uyeda, A., 2003. Carbon isotopic thermometry and geobarometry of sillimanite isograd in thermal aureoles: the depth of emplacement of upper crustal granitic bodies. *Contributions to Mineralogy and Petrology*, **154**, 534–549.
- van der Pluijm, B. A., Mezger, K., Cosca, M. A. & Essene, E. J., 1994. Determining the significance of high-grade shear zones by using temperature–time paths, with examples from the Grenville orogen. *Geology*, **22**, 743–746.
- Polyakov, V. B. & Kharlashina, N. N., 1995. The use of heat capacity data to calculate carbon isotope fractionation between graphite, diamond, and carbon dioxide: a new approach. *Geochimica et Cosmochimica Acta*, **59**, 2561–2572.
- Rathmell, M. A., Streepey, M. M., Essene, E. J. & van der Pluijm, B. A., 1999. Comparison of garnet–biotite, calcite–graphite, and calcite–dolomite thermometry in the Grenville Orogen, Ontario, Canada. *Contributions to Mineralogy and Petrology*, **134**, 217–231.
- Santosh, M. & Wada, H., 1993. Microscale isotopic zonation in graphite crystals: evidence for channeled CO₂ influx in granulites. *Earth and Planetary Science Letters*, **119**, 19–26.
- Satish-Kumar, M., 2000. Ultrahigh-temperature metamorphism in Madurai granulites, southern India: evidence from carbon isotope thermometry. *Journal of Geology*, **108**, 479–486.
- Satish-Kumar, M. & Wada, H., 2000. Carbon isotopic equilibrium between calcite and graphite in Skallen marbles, East Antarctica: evidence for the preservation of peak metamorphic temperatures. *Chemical Geology*, **166**, 173–182.
- Satish-Kumar, M., Santosh, M. & Wada, H., 1997. Carbon isotope thermometry in marbles of Ambasamudram, Kerala Khondalite Belt, Southern India. *Journal Geological Society of India*, **49**, 523–532.
- Satish-Kumar, M., Wada, H. & Santosh, M., 2002. Constraints on the application of carbon isotope thermometry in high- to ultrahigh-temperature metamorphic terranes. *Journal of Metamorphic Geology*, **20**, 335–350.
- Scheele, N. & Hoefs, J., 1992. Carbon isotope fractionation between calcite, graphite and CO₂: an experimental study. *Contributions to Mineralogy and Petrology*, **112**, 35–45.
- Sheppard, S. M. F. & Schwarcz, H. P., 1970. Fractionation of carbon and oxygen isotopes and magnesium between coexisting metamorphic calcite and dolomite. *Contributions to Mineralogy and Petrology*, **26**, 161–198.
- Spear, F. S., 1991. On the interpretation of peak metamorphic temperatures in light of garnet diffusion during cooling. *Journal of Metamorphic Geology*, **9**, 379–388.
- Thrower, P. A. & Mayer, R. M., 1978. Point defects and self-diffusion in graphite. *Physica Status Solidi (A)*, **47**, 11–37.
- Tracy, R. J., 1982. Compositional zoning and inclusions in metamorphic minerals. In: *Characterization of Metamorphism through Mineral Equilibria* (ed. Ferry, J. M.), *Reviews in Mineralogy*, **10**, 355–397. Mineralogical Society of America, Washington DC.
- Valley, J. W., 2001. Stable isotope thermometry. In: *Stable Isotope Geochemistry* (eds Valley, J. W. & Cole, D. R.), *Reviews in Mineralogy and Geochemistry*, **43**, 365–413. Mineralogical Society of America, Washington DC.
- Valley, J. W. & O’Neil, J. R., 1981. ¹³C/¹²C exchange between calcite and graphite: a possible thermometer in Grenville marbles. *Geochimica et Cosmochimica Acta*, **45**, 411–419.
- Wada, H., 1988. Microscale isotopic zoning in calcite and graphite crystals in marble. *Nature*, **331**, 61–63.
- Wada, H. & Suzuki, K., 1983. Carbon isotopic thermometry calibrated by dolomite–calcite solvus temperatures. *Geochimica et Cosmochimica Acta*, **47**, 697–706.

Received 6 August 2004; revision accepted 31 August 2005.